Quantum Signatures of the Optomechanical Instability

Jiang Qian,[1] A. A. Clerk,[2] K. Hammerer,[3] and Florian Marquardt[4,5]

[1]*Arnold Sommerfeld Center for Theoretical Physics, Center for NanoScience and Department of Physics,
Ludwig-Maximilians-Universität at München, Theresienstrasse 37, 80333 Munich, Germany*
[2]*Department of Physics, McGill University, Montreal, Quebec, Canada H3A 2T8*
[3]*Institute for Theoretical Physics, Institute for Gravitational Physics, Leibniz University Hanover,
Callinstrasse 38, D-30167 Hanover, Germany*
[4]*Institute for Theoretical Physics, Department of Physics, Friedrich-Alexander Universität Erlangen-Nürnberg,
Staudtstrasse 7, 91058 Erlangen, Germany*
[5]*Max Planck Institute for the Science of Light, Günter-Scharowsky-Straße 1/Bau 24, 91058 Erlangen, Germany*

In the past few years, coupling strengths between light and mechanical motion in optomechanical setups have improved by orders of magnitude. Here we show that, in the standard setup under continuous laser illumination, the steady state of the mechanical oscillator can develop a nonclassical, strongly negative Wigner density if the optomechanical coupling is comparable to or larger than the optical decay rate and the mechanical frequency. Because of its robustness, such a Wigner density can be mapped using optical homodyne tomography. This feature is observed near the onset of the instability towards self-induced oscillations. We show that there are also distinct signatures in the photon-photon correlation function $g^{(2)}(t)$ in that regime, including oscillations decaying on a time scale not only much longer than the optical cavity decay time but even longer than the mechanical decay time.

PACS numbers: 42.50.Wk, 07.10.Cm, 42.50.Lc, 42.79.Gn

By coupling optical and mechanical degrees of freedom, the emerging field of optomechanics provides exciting new opportunities to study the quantum mechanical behavior of macroscopic objects (for reviews, see Refs. [1,2]). Recent optomechanical cooling experiments are successfully bringing nanomechanical oscillators into their quantum mechanical ground state [3,4]. The same optomechanical coupling also promises the possibility of single-quadrature measurements of the resulting mechanical quantum states with the help of the light field [5–7]. For a reproducible and persistent quantum state, such measurements would result in an experimental determination of its full Wigner density via tomography, similar to what has been achieved in microscopic systems, for single ions or photons [8,9]. The recent advances in fabricating optomechanical devices have drastically improved coupling parameters, e.g., for optomechanical crystals [10], in microwave setups [3], and in other devices like GaAs disks [11] or toroidal optical microcavities [12]. It will likely be possible relatively soon to achieve optomechanical coupling strengths g_0 at the single-photon level that are comparable to the optical cavity decay rate κ, a feat that has already been achieved in cold atom optomechanical systems [13,14]. This regime of strongly nonlinear quantum optomechanics promises to pave the way towards generating and detecting novel quantum states in optomechanical systems. It is currently only beginning to be explored theoretically [15–17], although very early work already discussed quantum optomechanical effects in the (unrealistic) absence of any dissipation [18,19].

In the classical regime, nonlinear dynamics is known to occur when the system is driven by a blue-detuned laser.

When the input laser power crosses a certain threshold, the mechanical oscillator will undergo a Hopf bifurcation and start self-induced mechanical oscillations, a phenomenon termed ''parametric instability'' [20–25]. The quantum dynamics of this regime has first been studied in Ref. [15], and there is interesting synchronization behavior for arrays of coupled oscillators of this type [26].

In this Letter, we show that, for strong optomechanical couplings g_0 comparable to or greater than the optical decay rate κ and mechanical frequency ω_M ($g_0/\kappa \gtrsim 1$, $g_0^2/(\kappa \cdot \omega_M) \gtrsim 1$), a large laser driving, and an effectively zero temperature thermal bath, a nonclassical state of the mechanical oscillator with strongly negative Wigner density can be produced around the onset of self-induced oscillations. Because the state is time independent, one may use single-quadrature homodyne tomography to experimentally reconstruct its nonclassical Wigner density.

In addition, we propose to use the two-point photon correlation function $g^{(2)}(t)$ as an experimentally convenient probe for the peculiar quantum dynamics near the bifurcation. We identify two distinct signatures that enable experimentalists to reliably detect the onset and growth of the self-induced oscillation. We provide an explanation of the nonclassical decay of $g^{(2)}(t)$ in both the red- and blue-detuned regimes.

Within the rotating wave approximation, an optomechanical system can be described by the following standard Hamiltonian:

$$\hat{H} = \hbar[-\Delta + g_0(\hat{b}^\dagger + \hat{b})]\hat{a}^\dagger\hat{a} + \hbar\omega_M\hat{b}^\dagger\hat{b} + \hbar\alpha_L(\hat{a}^\dagger + \hat{a}) + \hat{H}_{\text{diss}}. \quad (1)$$

Here, $\hat{a}/\hat{b}$ are the operators for the photon/phonon modes, ω_M is the mechanical frequency, and α_L is the laser driving amplitude. $\Delta = \omega_L - \omega_C$ is the detuning of the laser from the cavity's *unperturbed* resonance (i.e., evaluated for zero mechanical displacement). g_0 describes the strength of the optomechanical coupling at the single-photon level.

When the dissipative terms in H_{diss} are taken into account, the density matrix $\hat{\rho}$ of the combined photon-phonon system evolves according to the quantum master equation:

$$\frac{d\hat{\rho}}{dt} = \mathcal{L}[\hat{\rho}] = \frac{[\hat{H}, \hat{\rho}]}{i\hbar} + \Gamma \mathcal{D}[\hat{b}, \hat{\rho}] + \kappa \mathcal{D}[\hat{a}, \hat{\rho}]. \quad (2)$$

Here, $\mathcal{L}$ is the quantum Liouville operator describing the time evolution of the density matrix $\hat{\rho}$, where we incorporate dissipation in the photon and phonon subsystems with decay rates κ and Γ, respectively. The standard Lindblad term is given by $\mathcal{D}[\hat{O}, \hat{\rho}] = \hat{O} \hat{\rho} \hat{O}^\dagger - \frac{1}{2}(\hat{O}^\dagger \hat{O} \hat{\rho} + \hat{\rho} \hat{O}^\dagger \hat{O})$. Note that we will assume zero bath temperature in our simulations, which will be reachable to a good approximation when GHz-frequency setups (e.g., optomechanical crystals) are deployed in dilution refrigerator settings. In this Letter, we are interested in the steady state solution of Eq. (2), where all the transient dynamics has died out. This is obtained numerically by finding the density matrix satisfying $\mathcal{L}[\hat{\rho}] = 0$ using the standard Arnoldi algorithm, as implemented in the ARPACK package. Due to its persistence, this state is ideal for making homodyne measurements of its mechanical Wigner density, in contrast to transient scenarios.

Specifically, we are interested in the mechanical Wigner density $W_M(x, p) = \frac{1}{\pi\hbar} \int_{-\infty}^{\infty} \langle x - y | \hat{\rho}_M | x + y \rangle e^{2ipy/\hbar} dy$, where $\hat{\rho}_M$ is the mechanical density matrix, obtained by tracing out the optical degrees of freedom from $\hat{\rho}$. The Wigner density is the quantum analog of the classical Liouville phase space probability density. A negative Wigner density is a strong signature of a nonclassical state. Early investigations [15] of the optomechanical instability in the regime around $g_0 \sim \kappa$ did not turn up nonclassical states.

In Figs. 1(a)–1(e), we show the overall properties of the steady state solutions. As we increase the laser detuning while keeping the input laser power fixed (points $A \rightarrow B \rightarrow C$), the phonon number in the mechanical oscillator rises sharply [plot (e)], signaling the onset of the self-induced oscillations. This is also reflected in the mechanical Wigner density $W_M(x, p)$. Below the onset (point A), $W_M(x, p)$ is a simple Gaussian, which starts to broaden just below the threshold, as the susceptibility of the system diverges and quantum fluctuations are strongly amplified (point B). Above the threshold, we have a coherent state undergoing circular motion in phase space but with an undetermined phase, which is the Wigner density observed at point C [15,17].

However, such a simple picture is inadequate for an optomechanical system with $g_0 \sim \kappa$, i.e., when one approaches the optomechanical instability deep in the quantum regime [27]. In such a system, we observe that, for a range of detuning Δ and laser driving α_L, the mechanical self-induced oscillation produces strongly nonclassical states with large negative areas in the Wigner density. This can be seen in the example of Fig. 1(d). Negative rims, shown in brighter color, develop at amplitudes slightly smaller than the average amplitude of oscillation. Plots (f)-(h) in Fig. 1 analyze negative states more deeply. In state D, (f) shows that the mechanical Fano factor $F = \frac{\langle \Delta n_b^2 \rangle}{\langle n_b \rangle}$ dips below the coherent state value 1, and its phonon number distribution (g) has a reduced variance. At larger coupling $g = 0.6\omega_M$ (h), the negative state exhibits a sharp peak and a smoother one, as opposed to a single broader peak of the non-negative state [28]. Overall, (f)-(h) show that the negative states are closer to a *single* Fock state *or* a superposition of a *few* Fock states, as compared with a coherent state [29]. Note, however, that the origin of this nonclassical state is *not* the same as that in the well-studied micromaser [30–33]. In the micromaser, the mechanism relies crucially on the swapping of a single excitation between an excited atom and a cavity over a fixed interaction time. These features are absent in our system.

Figure 1(i) maps out the regions in parameter space where negative Wigner densities occur. This "phase diagram" is shown as a function of the "quantum parameter" $\zeta = \frac{g_0}{\kappa}$ [15] and of the laser detuning $\Delta\omega_M$, at a fixed value of the laser driving strength α_L. It has been obtained by solving for the steady state of the optomechanical system under constant illumination, and the Wigner density is considered as nonclassical if a sufficiently large area turns out to be negative. The threshold criterion is a negative area of at least 3% of the positive area, the minimum value being at least 5% in the absolute value of the maximum. The numerical results shown here indicate that, for the parameters considered here, starting at $\frac{g_0}{\kappa} = 0.8$, the negative Wigner density states appear around detuning $\Delta/\omega_M = 0$, and a second negative Wigner density region opens up at $\frac{g_0}{\kappa} = 1.6$, around $\Delta/\omega_M = 0.9$ at the first blue sideband, where the instability is driven efficiently. The phonon number distribution displays a pronounced narrowing, getting closer to a single or a few mechanical Fock states. However, we find that many photon-phonon levels are still involved in the dynamics in the regime considered here, and there seems to be no simple explanation involving only a few levels.

These steady state nonclassical Wigner densities could be reconstructed via optomechanical quantum nondemolition quadrature detection [5,6] and subsequent quantum state tomography [34]. This merely involves illumination with another amplitude-modulated laser beam for readout, as explained in Ref. [6]. When observed, these would provide an accessible example of nonclassical states in a
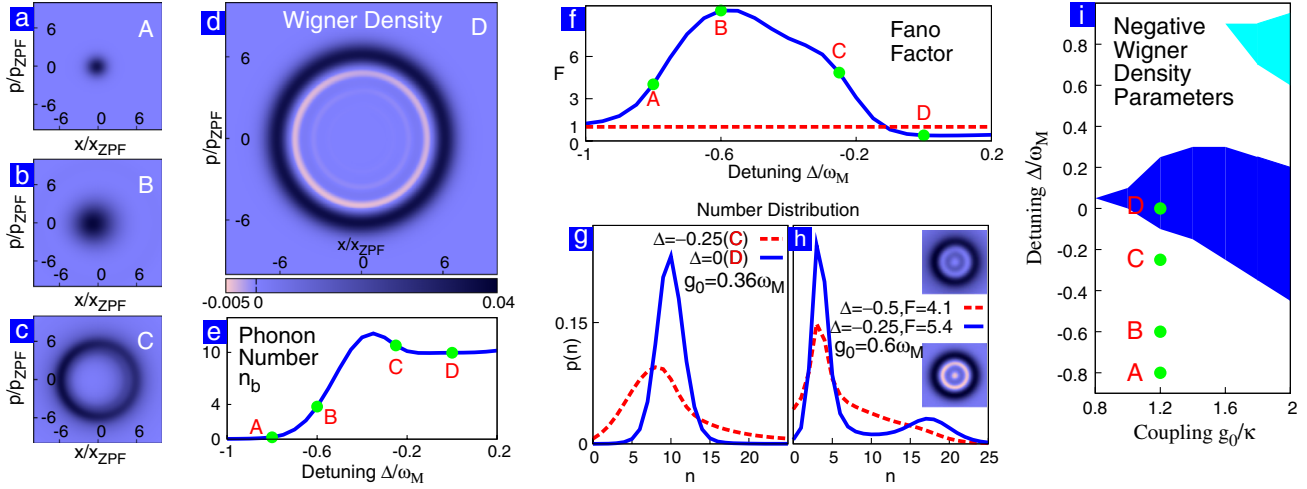
FIG. 1 (color online).   Nonclassical states in an optomechanical system. The laser input α_L is held constant, and the laser detuning Δ increases from the steady states A to D. The mechanical Wigner densities of these states are shown in (a)–(d). x_{ZPF} and p_{ZPF} are zero point fluctuations of the oscillator's position and momentum, respectively. Plot (e) shows the start of the self-induced oscillation, where the phonon number n_b of the oscillator rises quickly between states B and C. As the detuning further increases to D, a nonclassical mechanical quantum state with *negative* mechanical Wigner density state appears, as shown in (d). In (f), the evolution of the mechanical Fano factor F as a function of Δ is shown. It dips below the Poisson value 1 (the dashed line) in the nonclassical state shown here. In (g) and (h), we show that the negative Wigner density states have more sharply peaked phonon number distributions $p(n)$ compared with non-negative states. In (g), the $p(n)$ of states C and D [plots (c),(d)] are compared. In (h), where $g_0 = 0.6\omega_M$, the negative state (solid line) has two clear peaks in $p(n)$, in contrast to a single smooth peak for the non-negative state (dashed line). The Wigner densities of these two states are shown as insets. Finally, in (i), we show two regions in the parameter space of detuning Δ and coupling g_0, where significant negative Wigner density states exist. States A-D are indicated here. In all plots, other physical parameters are $g_0 = 0.36\omega_M$, $\kappa_M = 0.3\omega_M$, $\Gamma_M = 0.00147\omega_M$, and $\alpha_L = 0.311\omega_M$, except for (h), where $g_0 = 0.6\omega_M$ and $\alpha_L = 0.186\omega_M$. The intracavity photon number is $n_a \approx 0.1\text{--}0.7$ when $g_0 = 0.36\omega_M$, $-\omega_M \leq \Delta \leq 0$.

fabricated mesoscopic mechanical object. To date, there has been no experimental observation of nonclassical Wigner densities in the domain of micro- or nanomechanical structures. The experiment that came closest to that goal, and in the process did produce nonclassical mechanical Fock states, employed a complex multilayered superconducting circuit with piezoelectric coupling to a superconducting qubit and ultrafast pulse sequences [35]. Furthermore, in their setup, the resonator lifetime is too short to permit the reconstruction of the full Wigner density. By contrast, once optomechanical parameters can be improved to reach the single-photon strong coupling regime, the scheme discussed here would be relatively straightforward, being based on continuous laser illumination of an optomechanical setup whose fabrication is much less complex, as it involves only one material. Recently, a coupling $g_0/\kappa \approx 0.007$ has been achieved in an optomechanical crystal system [36], and further improvement is expected in that setup. In addition, there is the possibility that the parameters required here may be reached in cold atom optomechanical setups [13,14].

The full mechanical state reconstruction in the nonlinear quantum regime is an enticing and challenging goal. Nevertheless, it requires many experimental runs. It will be helpful to have other means of optically probing the quantum dynamics of the system around the onset of the

instability. A very suitable probe for the dynamics is provided by the two-point photon correlation function

$$g^{(2)}(t) = \frac{\langle \hat{a}_\tau^\dagger \hat{a}_{\tau+t}^\dagger \hat{a}_{\tau+t} \hat{a}_\tau \rangle}{(\langle \hat{a}_\tau^\dagger \hat{a}_\tau \rangle)^2}. \quad (3)$$

The angled brackets denote the average over $\hat{\rho}$. Here, we employ the two-point correlator for the intracavity photon field, extractable from our numerical simulations. However, we emphasize that it can be shown using input-output theory [37] that Eq. (3) also directly provides the $g^{(2)}$ function for the fluctuations of the output optical field.

In a steady state, $g^{(2)}$ does not depend on the initial time τ. Photon correlations are readily accessible in quantum optics experiments today with single-photon detectors (e.g., using a Hanbury Brown–Twiss setup), and they have been successfully employed to characterize the change of photonic statistics upon transmission through nonlinear systems. The most important example is photon antibunching in the resonance fluorescence of single-photon emitters, which has also recently been predicted to occur in optomechanical systems for sufficiently strong coupling [16].

As can be seen in Fig. 2, there are clear signatures in the photon correlator around the onset of parametric instability (point B). In particular, $g^{(2)}(t)$ persists at some value above
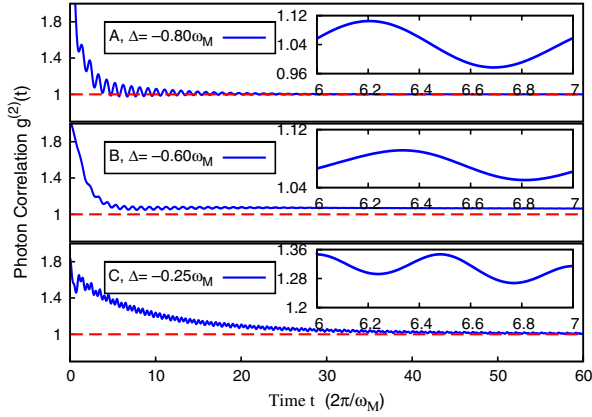
FIG. 2 (color online). Time dependence of photon-photon correlations near the regime of quantum optomechanical oscillations. *A*, *B*, and *C* label the same states as in Fig. 1. These plots show that there is a remarkably slow long-term decay near the onset of self-induced oscillations at point *B* (see the main text). The inset also shows the appearance of higher harmonics at point *C*.

unity over a very long time (middle panel, Fig. 2). It can be proven (see the Supplemental Material [37]) that, as long as the steady state of the system is not degenerate, we always have $g^{(2)}(t) \to 1 + \alpha \exp(-t/\tau_g)$ in the long-time limit $t \to \infty$. Here, the decay rate is $1/\tau_g = \mathrm{Re}(\lambda_1)$, where λ_1 is the eigenvalue of the Liouville operator $\mathcal{L}$ in Eq. (2) with the largest nonzero real part, characterizing the slowest decay in the system. This can be verified by plotting $\ln[g^{(2)}(t) - 1]$ to extract τ_g, which indeed agrees with the λ_1 obtained from $\mathcal{L}$ (see Fig. 3). As can be seen in the inset, τ_g rises strongly around the start of the self-induced oscillation (point *B*). This is connected to the fact that the overall mechanical damping rate goes to zero near the Hopf bifurcation [23].
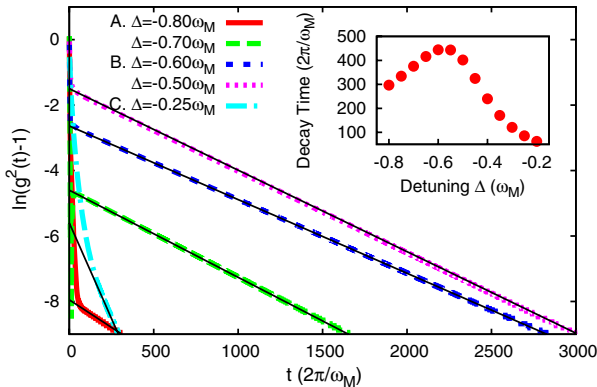

FIG. 3 (color online). Quantification of the slow approach of $g^{(2)}(t) \to 1$ near the onset of the self-induced oscillations, as observed in Fig. 2. $g^{(2)}(t) - 1$ obeys an exponential decay e^{-t/τ_g} in the long-time limit $t \to \infty$. The inset shows the decay time τ_g peaking toward very large values around point *B*, i.e., $\Delta = 0.6\omega_M$.

The second signature in $g^{(2)}$ is the appearance of higher harmonics when the self-induced oscillations are fully developed (see the insets of Fig. 2). To understand these in a semiclassical picture, we approximate the photon correlator via the classical intensity correlator, $\langle |\alpha(t + \tau)|^2 |\alpha(\tau)|^2 \rangle_\tau$. The light amplitude $\alpha(t) = e^{i\phi(t)} \sum_n \alpha_n e^{in\omega_M t}$ is modulated harmonically by the mechanical oscillations, as detailed in Ref. [23]. In the Supplemental Material [37], we show that a fully developed mechanical self-induced oscillation results in higher harmonics in $g^{(2)}$. To understand the *decay* of the resulting oscillations in the $g^{(2)}$, we take into account the mechanical phase diffusion induced by the radiation pressure shot noise [38]. presented the first analysis of the quantum contribution to phase diffusion in the parametric instability regime. Here, we follow a slightly modified approach. The phase fluctuates according to $\delta\phi(t) = (m\omega_M A)^{-1} \times \int_0^t dt' \delta F(t') \cos(\omega_M t')$, which yields

$$\mathrm{Var}[\delta\phi(t)] = \frac{1}{(m\omega_M A)^2} \frac{t}{4} [S_{FF}(\omega_M) + S_{FF}(-\omega_M)],$$

where S_{FF} is the force noise spectrum (see Ref. [39]). Thus,

$$\langle |\alpha(t + \tau)|^2 |\alpha(\tau)|^2 \rangle_\tau = \sum_{n=-\infty}^{+\infty} Z_n e^{in\omega_M t} e^{-n^2 \langle \delta\phi(t)^2 \rangle/2},$$

where $Z_n = |\sum_{m=-\infty}^\infty \alpha_m \alpha_{m-n}^*|^2$. This theory explains qualitatively the shape of the correlator even deep in the quantum regime (see the Supplemental Material [37]). Finally, we note that, in the red-detuned regime, the photon correlator decay can be described by the optomechanical cooling rate (see the Supplemental Material [37]).

To summarize, in this Letter, we investigated quantum signatures of light and mechanics for an optomechanical system in the parametric instability regime. We found that, at strong optomechanical coupling [$g_0 \sim \kappa$, $g_0^2 \sim (\kappa \cdot \omega_M)$], for a range of detuning and input power, the steady state mechanical Wigner density contains strong negative parts, signaling stable nonclassical states. Single-quadrature homodyne measurements can be used to reconstruct the Wigner density. In addition, the two-point photon correlator $g^{(2)}(t)$ displays two clear signatures near the onset of parametric instability. Finally, we explained the slow long-time decay of the photon correlations as due to the mechanical phase diffusion induced by photon shot noise. One should note that experimental observation of some of these photon correlation features does not require being in the nonlinear quantum regime and could succeed even in existing setups.

[1] F. Marquardt and S. M. Girvin, Physics **2,** 40 (2009).

[2] T. J. Kippenberg and K. J. Vahala, Science **321,** 1172 (2008).

[3] J. D. Teufel, T. Donner, D. Li, J. W. Harlow, M. S. Allman, K. Cicak, A. J. Sirois, J. D. Whittaker, K. W. Lehnert, and R. W. Simmonds, Nature (London) **475,** 359 (2011).

[4] J. Chan, T. P. M. Alegre, A. H. Safavi-Naeini, J. T. Hill, A. Krause, S. Groblacher, M. Aspelmeyer, and O. Painter, Nature (London) **478,** 89 (2011).

[5] V. B. Braginsky, F. Y. Khalili, and K. S. Thorne, *Quantum Measurement* (Cambridge University Press, Cambridge, England, 1995).

[6] A. A. Clerk, F. Marquardt, and K. Jacobs, New J. Phys. **10,** 095010 (2008).

[7] J. B. Hertzberg, T. Rocheleau, T. Ndukum, M. Savva, A. A. Clerk, and K. C. Schwab, Nat. Phys. **6,** 213 (2010).

[8] D. Leibfried, D. M. Meekhof, B. E. King, C. Monroe, W. M. Itano, and D. J. Wineland, Phys. Rev. Lett. **77,** 4281 (1996).

[9] A. I. Lvovsky, H. Hansen, T. Aichele, O. Benson, J. Mlynek, and S. Schiller, Phys. Rev. Lett. **87,** 050402 (2001).

[10] M. Eichenfield, J. Chan, R. M. Camacho, K. J. Vahala, and O. Painter, Nature (London) **462,** 78 (2009).

[11] L. Ding, C. Baker, P. Senellart, A. Lemaitre, S. Ducci, G. Leo, and I. Favero, Phys. Rev. Lett. **105,** 263903 (2010).

[12] E. Verhagen, S. Deléglise, S. Weis, A. Schliesser, and T. K. Kippenberg, Nature (London) **482,** 63 (2012).

[13] K. W. Murch, K. L. Moore, S. Gupta, and D. M. Stamper-Kurn, Nat. Phys. **4,** 561 (2008).

[14] F. Brennecke, S. Ritter, T. Donner, and T. Esslinger, Science **322,** 235 (2008).

[15] M. Ludwig, B. Kubala, and F. Marquardt, New J. Phys. **10,** 095013 (2008).

[16] P. Rabl, Phys. Rev. Lett. **107,** 063601 (2011).

[17] A. Nunnenkamp, K. Børkje, and S. M. Girvin, Phys. Rev. Lett. **107,** 063602 (2011).

[18] S. Mancini, V. I. Man'ko, and P. Tombesi, Phys. Rev. A **55,** 3042 (1997).

[19] S. Bose, K. Jacobs, and P. L. Knight, Phys. Rev. A **56,** 4175 (1997).

[20] V. Braginsky and A. Manukin, Sov. Phys. JETP **25,** 653 (1967).

[21] T. J. Kippenberg, H. Rokhsari, T. Carmon, A. Scherer, and K. J. Vahala, Phys. Rev. Lett. **95,** 033901 (2005).

[22] T. Carmon, H. Rokhsari, L. Yang, T. J. Kippenberg, and K. J. Vahala, Phys. Rev. Lett. **94,** 223902 (2005).

[23] F. Marquardt, J. G. E. Harris, and S. M. Girvin, Phys. Rev. Lett. **96,** 103901 (2006).

[24] M. Ludwig, C. Neuenhahn, C. Metzger, A. Ortlieb, I. Favero, K. Karrai, and F. Marquardt, Phys. Rev. Lett. **101,** 133903 (2008).

[25] I. S. Grudinin, H. Lee, O. Painter, and K. J. Vahala, Phys. Rev. Lett. **104,** 083901 (2010).

[26] G. Heinrich, M. Ludwig, J. Qian, B. Kubala, and F. Marquardt, Phys. Rev. Lett. **107,** 043603 (2011).

[27] Another necessary condition is that $g_0^2/(\kappa \cdot \omega_M)$ is not much smaller than 1.

[28] Note here that, due to the two-peak structure, the Fano factor of the negative Wigner density state remains above 1.

[29] D. A. Rodrigues and A. D. Armour, Phys. Rev. Lett. **104,** 053601 (2010).

[30] P. Filipowicz, J. Javanainen, and P. Meystre, J. Opt. Soc. Am. B **3,** 906 (1986).

[31] P. Meystre, G. Rempe, and H. Walther, Opt. Lett. **13,** 1078 (1988).

[32] J. Krause, M. O. Scully, and H. Walther, Phys. Rev. A **36,** 4547 (1987).

[33] B. T. H. Varcoe, S. Brattke, and H. Walther, J. Opt. B **2,** 154 (2000).

[34] A. I. Lvovsky and M. G. Raymer, Rev. Mod. Phys. **81,** 299 (2009).

[35] A. D. O'Connell, M. Hofheinz, M. Ansmann, R. C. Bialczak, M. Lenander, E. Lucero, M. Neeley, D. Sank, H. Wang, M. Weides, J. Wenner, J. M. Martinis, and A. N. Cleland, Nature (London) **464,** 697 (2010).

[36] J. Chan, A. H. Safavi-Naeini, J. T. Hill, S. Meenehan, and O. Painter, Appl. Phys. Lett. **101,** 081115 (2012).

[37] See Supplemental Material. at http://link.aps.org/supplemental/10.1103/PhysRevLett.109.253601 for the following details. In the first section we prove that the normalized photon correlation function of the output optical field is *idential* to the normalized intra-cavity optical correlation computed in the Eq. (3) in the main text. In the second section we prove that the photon correlation function always approaches one exponentially, with the decay rate stated in the main text. In the third section we prove that, in the semiclassical picture, the appearance of higher harmonics in the photon correlation function coincides with the start of the self-induced oscillation. Finally in the fourth section, we show that phase fluctuations can qualitatively account for the longtime decay of the photon correlation function in the blue-detuned regime, whereas optomechanical cooling can qualitatively account for the decay in the red-detuned regime.

[38] K. J. Vahala, Phys. Rev. A **78,** 023832 (2008).

[39] F. Marquardt, J. P. Chen, A. A. Clerk, and S. M. Girvin, Phys. Rev. Lett. **99,** 093902 (2007).